

附件四、國立臺灣大學研究成果專利構想揭露書

本校案號：061-141005
(由產學合作總中心填寫)

提案日期：中華民國 103 年 10 月 15 日

一、發明名稱	中文：電漿產生裝置 英文：Plasma Generation Device					
二、提案人	姓名	徐振哲	服務單位	化工系	職稱	副教授
	電話	02-3366-3034	e-mail	chsu@ntu.edu.tw		
三、權利歸屬	<input checked="" type="checkbox"/> 臺大 <input type="checkbox"/> 共有：與_____共有，共有比例為_____%：_____% (請填寫共有機構名稱) (臺大：共有機構) <input type="checkbox"/> 其他：_____					
四、本申請案是否已公開?	※根據中華民國及美國專利法規定，凡案件於申請前已見於刊物或公開發表(含學位論文口試、學位論文電子全文及電子書目資料(含摘要)上網、學位論文紙本全文上架、學術刊物發表、學術研討會發表、媒體報導、上課講習、公開演講、參加展覽會、競賽發表...等公開事項)，需於其事實發生後 <u>六個月內</u> (若申請美國案為 <u>12個月內</u>)提出申請方符合申請要件。					
	<input checked="" type="checkbox"/> 是(請續填以下) <input type="checkbox"/> 否，未來預計會公開(請續填以下) <input type="checkbox"/> 否 請註明公開事實及日期(若有多次公開，請條列) (1) 期刊發表：Analytical Chemistry, vol. 86, p. 8757, 7/23/2014 (2) 公開演講：IUMRS 會議發表, 8/28/2014 (3) 公開演講：VASSCAA 會議發表, 10/7/2014 ※學位論文口試視同公開，若採取以下手段，則可能認為不算公開(1)口試會議不以網路公告(2)口試時關門不讓聽眾自由進出，避免對不特定人士揭露技術(3)所有參加口試會議者簽署保密同意書(若有簽屬請提供影本一份)。 ※學位論文繳交提醒：論文電子全文、電子書目資料(含摘要)及紙本論文若於網路上或圖書館供人查詢或閱覽也算是公開，若欲採取保密措施需於(1)本校電子學位論文服務系統上傳論文電子全文時，於系統上勾選 <u>電子全文延後公開</u> ，並另行填寫「學位論文延後公開申請書」向圖書館申請(2) <u>電子書目資料(含摘要)</u> 及(3) <u>紙本論文延後公開</u> (注意：若於公開後才向圖書館申請延後公開，則仍以原公開日期為公開日)。 ※為維持申請專利內容之新穎性，請盡量在申請前勿公開相關內容。若已公開或預計公開請檢附已公開或預計公開之相關文件。					
五、建議檢索關鍵字	中文：微電漿，可撓式 英文：microplasma, flexible					

※發明人欄位填寫說明：

- (1)發明人超過三位時，請自行複製發明人欄位使用。
- (2)發明人請填寫實際的發明人，參酌美國專利實務上的認定，所謂發明人必須是對發明概念之形成及至少一項申請專利範圍之標的有所貢獻之人，才能稱為發明人。美國專利法規定，若列名之發明人未有發明之事實，則不得取得專利；若發明人記載錯誤，且可證明有「欺瞞之意圖」，則此專利權無法主張權利（單純接受指示，依所設計之實驗完成實驗結果者、提出需求者、提出產品缺點者等無實質貢獻者，不能算是發明人）。
- (3)未來收益分配之有功人員不限於此專利申請案所列之實際發明人。

六、發明人

1	姓名	(中文/英文)徐振哲/Cheng-che Hsu		
	服務單位	台灣大學	服務單位	台灣大學
	國籍	<input checked="" type="checkbox"/> 中華民國 <input type="checkbox"/> 其他：_____	身份證字號 或護照字號	A121837437
	e-mail	chsu@ntu.edu.tw	e-mail	chsu@ntu.edu.tw
	聯絡地址	台北市羅斯福路四段一號		

2	姓名	(中文/英文)楊曜禎/Yao-jhen Yang		
	服務單位	台灣大學	職稱	學生
	國籍	<input checked="" type="checkbox"/> 中華民國 <input type="checkbox"/> 其他：_____	身份證字號 或護照字號	L123965068
	e-mail	f98524038@ntu.edu.tw	電話	02-3366-9751
	聯絡地址	台北市羅斯福路四段一號		

3	姓名	(中文/英文)高鵬凱/Peng-kai Kao		
	服務單位	台灣大學	職稱	學生
	國籍	<input checked="" type="checkbox"/> 中華民國 <input type="checkbox"/> 其他：_____	身份證字號 或護照字號	A127724957
	e-mail	pengkaikao@gmail.com	電話	02-3366-9751

	聯絡地址	台北市羅斯福路四段一號		
--	------	-------------	--	--

4	姓名	林子軒		
---	----	-----	--	--

	服務單位	台灣大學	職稱	學生	CONFIDENTIAL
	國籍	<input checked="" type="checkbox"/> 中華民國 <input type="checkbox"/> 其他：_____		身份證字號 或護照字號	P123571872
	e-mail	ooxx_ck0608@hotmail.com		電話	02-3366-9751
	聯絡地址	台北市羅斯福路四段一號			
5	姓名	王誌君			
	服務單位	台灣大學	職稱	學生	
	國籍	<input checked="" type="checkbox"/> 中華民國 <input type="checkbox"/> 其他：_____		身份證字號 或護照字號	R123744242
	e-mail	gn01159472@hotmail.com		電話	02-3366-9751
	聯絡地址	台北市羅斯福路四段一號			
七、專利類別	<input checked="" type="checkbox"/> 發明 <input type="checkbox"/> 新型 <input type="checkbox"/> 新式樣(新專利法將改為設計專利) ※發明，指利用自然法則之技術思想之創作。 新型，指利用自然法則之技術思想，對物品之形狀、構造或裝置之創作。 新式樣，指對物品之形狀、花紋、色彩或其結合，透過視覺訴求之創作。 ※請注意：美國無新型專利，若勾選新型，亦將提出發明專利申請。				
八、申請國家及理由	<input checked="" type="checkbox"/> 中華民國 <input checked="" type="checkbox"/> 美國 <input type="checkbox"/> 其他：_____ ※本校專利申請審查原則：以中華民國、美國兩國為優先考量，若欲申請其他國別(含歐盟、PCT)，則需請發明人依擬申請之國別提供以下三種狀況之說明文件：(1)有廠商願意技術移轉(2)有授權潛力(3)市場評估良好，並經校方審查程序，如未附相關資料則無法審查。				
九、本申請案所屬技術領域別與可能應用範圍	本申請案所屬技術領域	電漿設備，電漿鍍膜，表面處理			
	可能應用範圍(產業或產品)	殺菌、表面處理、電漿光譜分析裝置等需要產生電漿之系統中均可適用。			
	※本專利應用之可行性及潛在授權廠商： (1)本專利之技術與該國現有產品或技術之競爭性如何？ (2)依據本專利之產品或製程進入該國市場的可行性如何？ (3)若有任何公司曾與您接洽或詢問過相關技術，亦請提供。				
	申請國家	應用可行性及潛在授權廠商建議(請以文字說明)			
	中華民國	殺菌、表面處理、電漿光譜分析裝置等需要產生電漿之系統中均可適用。			
	美國	殺菌、表面處理、電漿光譜分析裝置等需要產生電漿之系統中均可適用。			
	其他：_____				

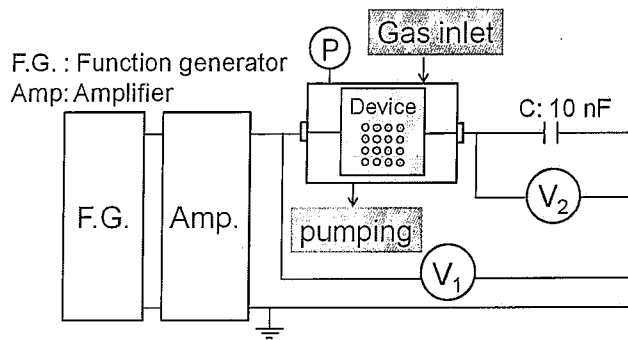
※申請「後期專利申請案」但已提出「先期專利申請案」者，可直接跳至最後一頁，考慮填寫附件四。

十、發明背景及內容	<p>(1) 發明所欲解決之問題：係指申請專利之發明或新型所要解決先前技術中存在的問題。(此欄位亦可見於技術推廣表『業界的技術困擾』)</p> <p>1. 一般微電漿產生裝置大多使用不可撓曲之基材(如矽基板、玻璃)，使微電漿的應用受到了限制，不能應用至非平面的情況。</p> <p>2. 微電漿產生裝置的金屬電極層經常需使用真空的鍍膜技術，提高電漿產生裝置成本。</p> <p>3. 微電漿產生裝置的金屬電極層圖案化多倚靠半導體製程技術中的微影製程。微影製程雖能在電極的圖案化上提供較佳的解析度，但因為需要無塵室的設備，使得微電漿產生裝置的成本高而不能將微電漿技術普及應用。</p>
	<p>(2) 解決問題之技術手段：即欲獲得專利保護之主要技術特徵，請條列本案相較於先前技術具有創新、進步或功效等獨特技術部分，做為撰寫申請專利範圍之參考。</p> <p>本發明包含</p> <p>1. 使用已商業化之軟性印刷電路板雙面板做為電漿產生裝置之基底。此種電路板之結構為一介電層，其兩側鍍上銅金屬，可省去高成本之金屬電極鍍膜製程。此外，此種電路板因已被廣泛使用，因此取得容易，成本低廉。</p> <p>2. 以「印表機碳粉轉印技術」進行金屬電極圖案化製程。藉由此種技術，僅需使用辦公室用品，即可在一般實驗室進行此製程，如此，對於金屬電極上之圖案，能較有彈性地依使用者之需求做變化。</p> <p>3. 電漿驅動之電源可為直流、交流、脈衝式直流，或脈衝式交流</p> <p>4. 電漿氣體可使用包括，但不限於，空氣、氫氣、氬氣、氮氣等氣體。同時，也可依照需求，在氣氛中添加反應先驅物，利用電漿高反應性之特性在電漿區進行反應。</p>
	<p>(3) 對照先前技術之功效：係指前述技術手段所產生的技術效果。</p>

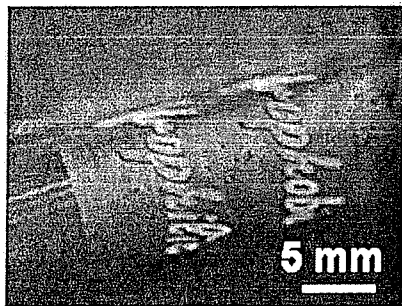
使用上述揭露之技術，能製備出可撓式電漿產生裝置。電漿產生裝置之區域可被使用者喜好定義。電漿系統示意圖如圖一所示。

圖二所示為此電漿產生裝置於在纏繞在外徑為5 mm之玻璃管外，在氫氣氣氛中，以450 V(方均根值)、10 kHz電源驅動所生成之穩定電漿放電之外觀圖。

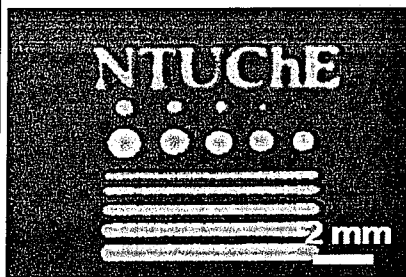
圖三所示為定義有「NTUCHE」、直徑160至1100微米之圓、以及寬度250至600微米長方形之電漿產生裝置以450 V(方均根值)、10 kHz電源驅動所產生電漿之外觀圖。



圖一



圖二

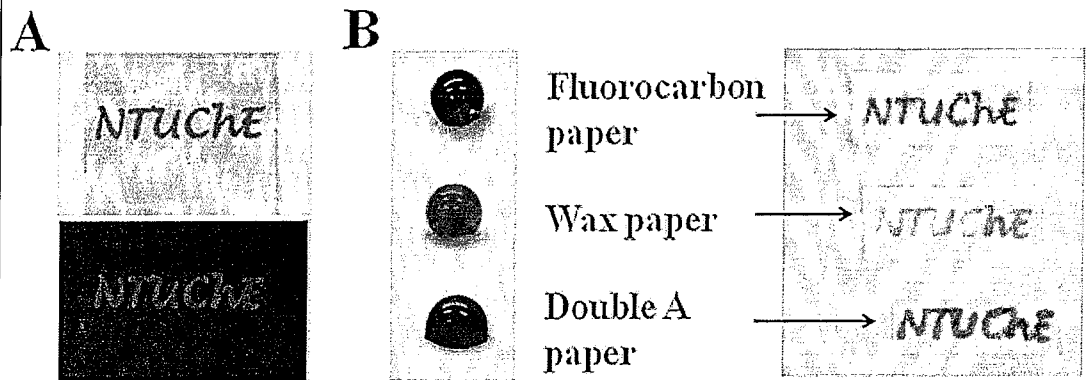


圖三

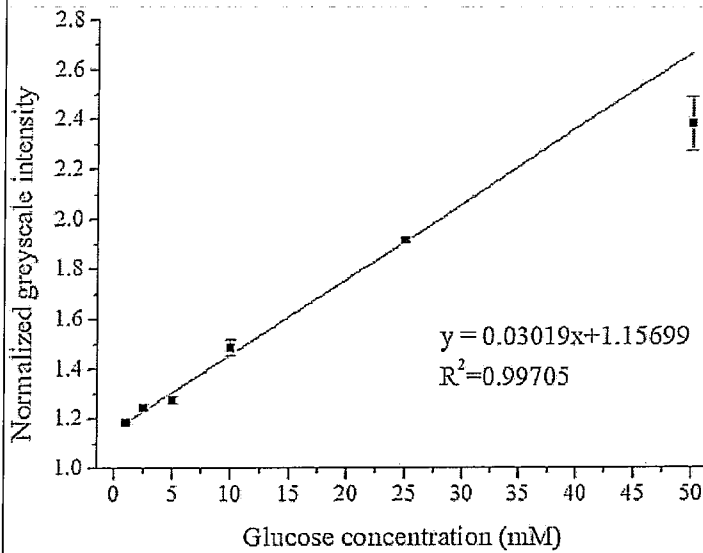
十一、本發明之實施方式

※請舉出至少一項關於本發明之較佳實施方式或具體實施例，可配合圖示說明，使所屬技術領域中具有通常知識者能了解其內容並可據以實施。(本項可於本表格說明或以技術文件、論文等代替)

將經過特殊處理、疏水之紙張與電漿產生裝置緊密貼合，於空氣的氮氣中對電漿產生裝置(圖四 (A))施以 2 kV, 45 kHz 之交流電壓，進行在疏水之紙張上產生親疏水之對比之圖案化製程。圖四(B)顯示不同的疏水紙張經電漿處理後，染料水溶液在紙張上所呈現與電漿產生區域一致之親水圖案。利用此製程，吾人可在利用疏水之紙張與此電漿裝置製作紙基微流道裝置，並應用於生物感測。圖五為利用此種技術所製備出生物感測元件於葡萄糖濃度檢測之應用，x 軸為葡萄糖濃度，y 軸為葡萄糖與偵測用試劑反應後所產生之顯色反應，經圖案灰階化後之量化數值。



圖四



圖五

附件五、相關文獻陳報表

※請條列與本案技術領域相關之文獻，包含但不限於提案人或發明人之相關專利、論文等。

1. 專利(包含申請中及已獲證案件，請至少寫出申請國別及申請案號/獲證號)
 - (1)
 - (2)
2. 其他(該文獻若無法於網路上輕易取得，請檢附相關文件影本 1 份)
 - (1) S. J. Park, C. J. Wagner, C. M. Herring, J. G. Eden, Flexible microdischarge arrays: Metal/polymer devices. Appl. Phys. Lett. 77, 199-201 (2000); published online EpubJul (10.1063/1.126923).
 - (2) J. D. Readle, K. E. Tobin, K. S. Kim, J. K. Yoon, J. Zheng, S. K. Lee, S. J. Park, J. G. Eden, Flexible, Lightweight Arrays of Microcavity Plasma Devices: Control of Cavity Geometry in Thin Substrates. IEEE Trans. Plasma Sci. 37, 1045-1054 (2009).
 - (3) M. Lu, S. J. Park, B. T. Cunningham, J. G. Eden, Microcavity plasma devices and arrays fabricated by plastic-based replica molding. J. Microelectromech. Syst. 16, 1397-1402 (2007).
 - (4) M. Abdelgawad, A. R. Wheeler, Rapid Prototyping in Copper Substrates for Digital Microfluidics. Adv. Mater. 19, 133-137 (2007).
 - (5) P. K. Kao, C. C. Hsu, Battery-Operated, Portable, and Flexible Air Microplasma Generation Device for Fabrication of Microfluidic Paper-Based Analytical Devices on Demand. Anal. Chem. 86, 8757-8762 (2014)
 - (6) 高鵬凱，「利用電漿製程製備紙為基底之微流道裝置」，碩士論文，台灣大學，2014。

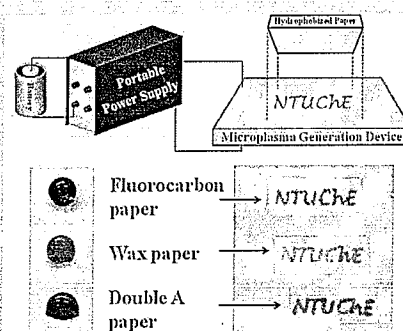
Battery-Operated, Portable, and Flexible Air Microplasma Generation Device for Fabrication of Microfluidic Paper-Based Analytical Devices on Demand

Peng-Kai Kao and Cheng-Che Hsu*

Department of Chemical Engineering, National Taiwan University, Taipei, 10617, Taiwan

S Supporting Information

ABSTRACT: A portable microplasma generation device (MGD) operated in ambient air is introduced for making a microfluidic paper-based analytical device (μ PAD) that serves as a primary healthcare platform. By utilizing a printed circuit board fabrication process, a flexible and lightweight MGD can be fabricated within 30 min with ultra low-cost. This MGD can be driven by a portable power supply (less than two pounds), which can be powered using 12 V-batteries or ac-dc converters. This MGD is used to perform maskless patterning of hydrophilic patterns with sub-millimeter spatial resolution on hydrophobic paper substrates with good pattern transfer fidelity. Using this MGD to fabricate μ PADs is demonstrated. With a proper design of the MGD electrode geometry, μ PADs with 500- μ m-wide flow channels can be fabricated within 1 min and with a cost of less than \$USD 0.05/device. We then test the μ PADs by performing quantitative colorimetric assay tests and establish a calibration curve for detection of glucose and nitrite. The results show a linear response to a glucose assay for 1–50 mM and a nitrite assay for 0.1–5 mM. The low cost, miniaturized, and portable MGD can be used to fabricate μ PADs on demand, which is suitable for in-field diagnostic tests. We believe this concept brings impact to the field of biomedical analysis, environmental monitoring, and food safety survey.



Microfluidic paper-based analytical devices (μ PADs) have recently gained significant attention for potential applications in general healthcare,^{1–4} immunochemical assays,⁵ biochemical analysis,⁶ environmental monitoring,^{7,8} and food safety.⁹ For a μ PAD, the paper substrate was patterned into regions of hydrophilic channels demarcated by hydrophobic barriers. Compared with conventional glass-based or polydimethylsiloxane-based microfluidics, μ PADs are great candidates as point-of-care diagnostic tools with advantages of low cost, fast response, facile interpretation, simple disposal, and no pumps being required to transport the fluids on a porous paper substrate due to capillary action.¹⁰ A promising paper-based microfluidic device was first developed by the Whitesides group using the photolithography process.⁶ Since that time, there has been a great number of literature reporting different fabrication techniques, such as plasma etching,¹¹ plasma polymerization,¹² wax printing,^{13,14} inkjet printing,¹⁵ contact printing,¹⁶ flexographic printing,¹⁷ plotting,¹⁸ cutting,¹⁹ and drawing.²⁰ Jet-type plasma sources²¹ with an ultrathin nozzle can potentially be used for μ PAD fabrication. Although several of the above processes offer advantages of low cost and possibility for large scale fabrication, it is required to manufacture the μ PADs in the laboratory and then ship the devices to a designated location. For applications such as in-field diagnostics, fabrication of μ PADs on site or on-demand offers great advantages. Under this circumstance, a facile and low-cost process that possesses good pattern transfer fidelity

and is operated using portable and battery-powered equipment is highly desired.

Atmospheric-pressure (AP) microplasmas²² are plasmas operated under 1 atm with at least one geometric dimension confined to 1 mm or less. According to the “*pd* scaling” of the Paschen curve, a sufficiently small distance gap results in stable glow discharges generated by reasonably low applied voltage at 1 atm.²² In addition, the miniaturized dimension offers a locally highly reactive environment with high power density but small total power consumption. These features enable AP microplasma to be utilized in various applications, such as maskless patterning,^{23,24} biomedical applications,²⁵ optical spectroscopy, and mass spectrometry.^{26,27} Due to their sub-millimeter miniaturized size, microplasma generation devices (MGDs) are most often fabricated using semiconductor fabrication processes such as lithographic and/or vacuum-based processes, which are expensive and time-consuming. Using a screen print-based process to fabricate MGDs has recently been reported.²⁸ This process offers advantages of low cost and high accessibility, but it requires several hours to fabricate a MGD. For the MGD to be utilized as a tool to fabricate μ PADs, a low-cost and rapid process to fabricate MGDs is highly desired.

Among several types of AP microplasma systems reported in the literature,^{29,30} dielectric barrier discharge (DBD) is one

Received: May 26, 2014

Accepted: July 23, 2014

Published: July 23, 2014

type that has been widely utilized. A DBD-type system consists of one or more dielectric layers located between two electrodes. The existence of the dielectric layer effectively prevents the formation of arc discharge and enables the formation of spatially uniform low temperature (near room temperature) plasmas with low power consumption. Based on these characteristics, DBDs have been widely employed in ozone generation, surface treatment, and gas decomposition or reforming.^{31,32} In this work, we report the development of a low-cost DBD-type MGD that can be fabricated in a simple, efficient, and cost-effective manner. This MGD can be operated in ambient air and is battery powered. A facile and low cost process using this MGD to fabricate μ PADs is demonstrated. Finally we test the μ PADs by performing quantitative colorimetric assays and establish calibration charts for detection of glucose and nitrite. The impact using this portable MGD-based μ PAD fabrication process in in-field diagnostic tests will be discussed.

EXPERIMENTAL SECTION

Fabrication of μ PADs. AP MGD. Figure 1A shows a photograph of the battery-operated, portable MGD. This system consists of a high-voltage ac power supply (PVM12, Information Unlimited, USA) and a MGD. The ac power source requires 12 V dc input, which can be either batteries (e.g., A23, Sony, as shown in this figure) or using an ac–dc converter. We note that the use of a 12 V battery to drive this ac power source offers great possibilities when the MGD is used in the field. For example, lead-acid rechargeable batteries for automobiles are able to deliver dc 12 V. A battery with a capacity of 45 amp-hour is sufficient to supply the MGD operation for at least 20 h. In this work, an ac–dc converter is used to fabricate the μ PADs. The power source delivers ac voltages with a frequency between 20 and 50 kHz and a voltage up to 15 kV. We note that the amplitudes of the ac voltages reported in this work are all peak-to-peak voltages. The MGD is fabricated using a modified printed circuit process based on the toner transfer method. The fabrication process defines patterns on a double-sided copper clad laminate (CCL), with the detail illustrated in Supporting Information Figure S1. With this process, MGDs can be fabricated within 30 min. Figure 1B shows the schematic of the experimental setup. A 1.02-k Ω ballast resistor was connected in series with the MGD to limit the current to elongate the MGD lifetime. A voltage probe (HVP-18HF, PINTEK) was used to monitor the voltage across the MGD. Figure 1C shows the visual appearance of the MGD when the plasma is ignited in the ambient air with a voltage of 2.0 kV and 45 kHz when the ac power source is driven by a 12 V battery. The use of a proper applied voltage is one critical factor for the MGD operation. A test operating the MGD using various applied voltages was performed, and the results were shown in Supporting Information Figure S2. Based on the results, an applied voltage of 2.0 kV is chosen for the MGD operation throughout this work, unless otherwise specified.

Hydrophobic Paper Substrate. In this work, three different types of hydrophobized paper were utilized as the paper substrate for the fabrication of μ PADs to demonstrate the process viability and flexibility. The first type, fluorocarbon paper, is the filter paper (ADVANTEC grade 2) coated by fluorocarbon utilizing plasma polymerization with a low pressure plasma system. The fluorocarbon plasma polymerization was performed using a parallel-plate capacitively coupled system under the following conditions: $c\text{-C}_4\text{F}_8$ (1 sccm)/Ar (50

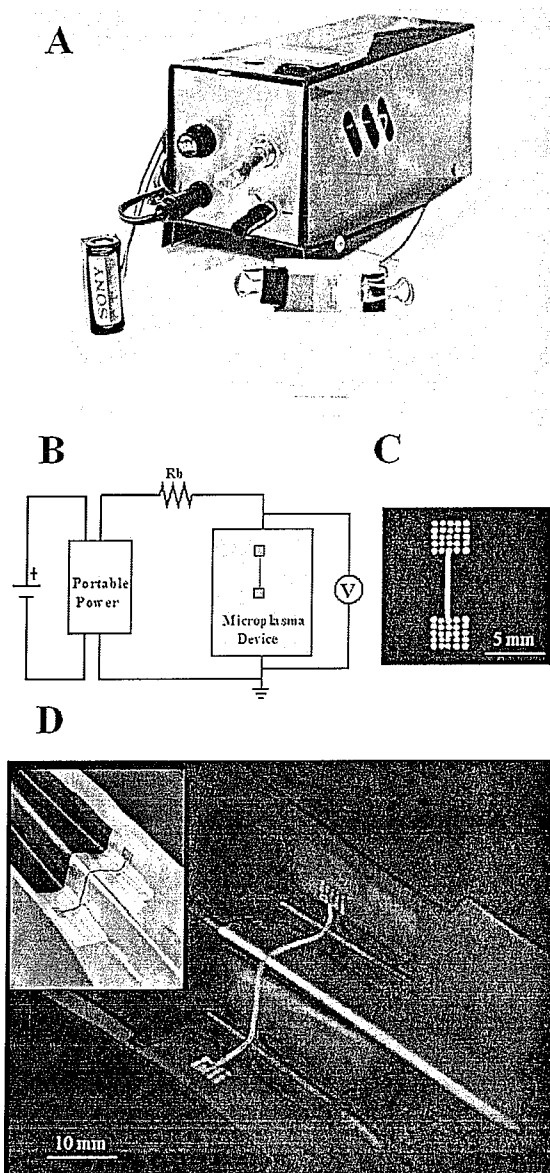


Figure 1. (A) Photograph of the experimental setup. (B) Schematic of the experimental setup. (C) Visual appearance of the MGD ignited in the ambient air with a voltage of 2.0 kV and 45 kHz with the power source driven by a 12 V battery. (D) Photograph of a folded MGD with plasma ignited with a voltage of 2.2 kV and 45 kHz. The inset shows the visual appearance of the MGD when plasma is not ignited.

sccm), 13.56 MHz RF power 30 W, and 20 s processing time. The second type of hydrophobized paper, wax paper, is filter paper coated with wax. To prepare this type of hydrophobic paper, filter paper (ADVANTEC grade 2) was dipped in a heptane solution containing paraffin wax (6 g/L) for 10 s and removed and placed in a fume hood to allow evaporation of heptane. The paper samples were then placed on a hot plate at 80 °C for 10 min to cure the wax. The third type of paper, Double A paper, is commercially available copy paper (Double A, 80 gsm). Such a type of paper typically contains internal sizing agents and CaCO_3 , in addition to cellulose. The addition of sizing agents makes the paper fiber hydrophobic and

enhances the paper printability. Alkyl ketene dimer (AKD), for example, is one widely used internal sizing agent in the paper industry. AKD reacts with the hydroxyl functional groups of cellulose and forms a β -keto-ester. These hydrocarbon chains thus impart hydrophobicity to cellulose fiber.^{33,34}

Microfluidic Channels Formation and Channel Shape Examination. The hydrophilic channels on the above-mentioned hydrophobic paper substrates were fabricated by having the hydrophobized paper face and firmly attach to the surface of the MGD device. The fluorocarbon paper, wax paper, and Double A paper were then treated using the plasma generated on the surface of the MGD with a voltage of 2.0 kV and 45 kHz for 15, 30, and 3 s, respectively, unless otherwise specified. The treatment time for three different kinds of paper is determined experimentally and is the minimal time duration required to pattern a complete hydrophilic channel for fluid flow. The significantly different time durations are due to different hydrophobic material compounds and their amounts (for example, thickness). For example, wax paper has relatively thicker paraffin and requires the longest treatment time to define the hydrophilic channel. Proper selection of the applied voltage and the process time of this MGD-based process is the key to obtain μ PADs with desired performance, as demonstrated in Supporting Information Figure S3. For experimental sets to examine the channel shape and width, orange II dye solution was introduced to the hydrophilic channels and the channel shape and width can be clearly visualized. For all tests unless otherwise specified, wax paper was chosen as the hydrophobic paper as the substrate to fabricate μ PADs. The microfluidic channel fabricated on wax paper by MGD with an applied voltage of 2.0 kV and 45 kHz for 30 s shows a channel depth of $56.8 \pm 6.1 \mu\text{m}$. Such a channel depth together with a typical channel width of $351.6 \pm 28.6 \mu\text{m}$ yields an aspect ratio (height to width) of 0.16. Given the lateral and vertical diffusion of the reactive species and the limitation of the MGD fabrication process, the smallest trench width that can be fabricated in this process is about $350 \mu\text{m}$. The total cost to fabricate μ PADs is well below \$USD 0.05/device, including the cost for MGD fabrication, chemicals and materials used, and MGD operation, as detailed in Supporting Information Table S1.

Chemicals. The following chemicals were purchased from commercial suppliers (Sigma-Aldrich, Acros) and used as received without further purification: acetone, iron(III) chloride, paraffin wax, *n*-heptane, orange II, D-(+)-glucose, potassium iodide (99.5%), trehalose (98.5%), monosodium phosphate, disodium phosphate, glucose oxidase, horseradish peroxidase, sodium nitrite (99%), *N*-(1-naphthyl)ethylenediamine (98%), sulfanilamide (99%), and citric acid (99.5%). All aqueous solutions were prepared using deionized water.

Colorimetric Assays. In this work, glucose and nitrite assays were tested to confirm that the fabricated μ PAD is capable to be used in quantitative analyses. The glucose assay was based on those previously reported.^{6,35,36} The glucose indicator was prepared by spotting two solutions on top of the detection region. Solution 1 contains 0.6 M potassium iodide and 0.3 M trehalose in a 100 mM phosphate buffer at pH 6.4. Solution 2 contains 5:1 glucose oxidase (120 units/mL) and horseradish peroxidase (30 units/mL). First, 0.2 μL of solution 1 was applied to the detection region and allowed to dry for 3 min. Then, 0.2 μL of solution 2 was spotted on top of the detection region and allowed to react for another 3 min. Next, 1

μL of D-(+)-glucose solution was added to the sample zone. The μ PAD was then placed in a confined humid chamber for 15 min, allowing the enzymes to metabolize the glucose and to form yellow or brown chromogen product. According to Klasner et al.,³⁵ the humid atmosphere ensures that all channels are wet and thus have enough time for product generation (iodine). Finally, the μ PAD was removed out of the humid ambient and allowed to dry at room temperature prior to taking a photo image and scanning.

The NO_2^- stock solution was prepared by dissolving sodium nitrite in deionized water. The nitrite indicator contains 10 mM *N*-(1-naphthyl)ethylenediamine, 50 mM sulfanilamide, and 330 mM citric acid.³⁷ First, 0.2 μL of the nitrite indicator was spotted in the detection region and allowed to react for 3 min. Then, 1 μL of the nitrite stock solution was spotted on the sample zone. The devices were placed and allowed to dry at room temperature for 5 min before taking the photo image as well as scanning.

Image Processing. To quantify the color response, a commercially available scanner (HP, Deskjet F4280 Printer) was used to capture the visual readouts of the colorimetric assays. The scanned image was then deconvoluted using the color image obtained from the detection region into red (R), green (G), and blue (B) components. Two processing schemes using these RGB components were performed to quantify the color image. For the glucose assay, we applied the first scheme, which summarizes the normalized RGB components, as an indicator of the "brightness" of the image. This scheme weighs RGB components equally and is somewhat different from the gray scale, which weighs RGB components differently. As for the nitrite assay, we applied the second scheme, which takes the ratio of $R/(R+G+B)$ as the quantification, since the colorimetric output produced from the nitrite assay is a red-violet azo compound.³⁷

RESULTS AND DISCUSSION

Flexibility of the MGD. Figure 1D shows the visual appearance of the MGD operated in ambient air under a folding configuration. This demonstrates a key feature of the MGD: flexibility. Such a feature allows for treating a curved or nonflat surface; it also extends the nature of this surface treatment process from 2-dimensional to 3-dimensional and offers great possibilities in various applications where treating nonflat surfaces is desired.

Hydrophilic Trenches on Hydrophobized Paper Substrates. Making hydrophilic trenches on three types of hydrophobized paper substrates, namely fluorocarbon paper, wax paper, and Double A paper, was demonstrated as the first test in utilization of the MGD-based process to fabricate μ PADs. Figure 2A shows the visual appearance of the MGD (upper image) and the plasma generated with this device (lower image) with a specially designed NTUChE-shaped geometry on the MGD. Before MGD treatment, the images with a colored droplet on the surface of three types of hydrophobized paper are shown in the left panel of Figure 2B. It clearly shows the hydrophobic nature with contact angles of 136.9, 124.4, and 108.8° on fluorocarbon paper, wax paper, and Double A paper, respectively. After the hydrophobized paper substrates were treated by MGD, all paper substrates form hydrophilic NTUChE-shaped channels on the surface, as depicted in the right panel of Figure 2B. We note that utilizing Double A paper as the paper substrate for μ PADs provides great convenience and opportunities because paper of this type

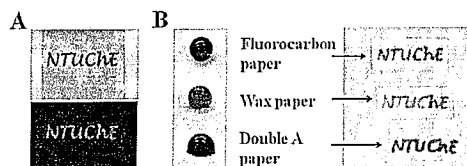


Figure 2. (A) Visual appearance of the MGD (upper panel) and the MGD with plasma ignited (lower panel). This MGD is fabricated with a specially designed NTUCHE-shaped geometry. (B) Three types of hydrophobized paper: fluorocarbon paper, wax paper, and double A paper before and after treatment with MGD with a voltage of 2.0 kV and 45 kHz for 15, 30, and 3 s, respectively. All paper substrates forming hydrophilic NTUCHE-shaped channels on the surface are shown.

is itself hydrophobic and easily accessible and no further hydrophobized process is required.

The plasma ignited by the MGD operated in air is able to generate multiple reactive species, which react with paper substrates, and a substantial increase in surface energy of surfaces occurs.³² Surfaces with high surface energy are typically more hydrophilic; therefore, hydrophilic microfluidic channels on top of the hydrophobic paper substrates are achieved. Such a plasma treatment process results in surface modification of paper substrates in a designated area without making a visible mark on the treated surface, which retained its flexibility as noted above.

MGD Pattern-Design and Channel Characteristics. For this present MGD, plasmas are formed at the edge of the patterns. The area of the paper surface being treated is confined

to the plasma-generated area. To fabricate μ PADs with desired channel geometries, a careful design of the MGD is desired. To demonstrate how the geometry of the plasma ignited on the MGD is transferred to the μ PADs, MGDs with various geometries were fabricated and corresponding channel shapes were examined. Figure 3 shows 3 sets of tests made by three specially designed patterns. Figure 3A shows the MGD pattern with two $2.5 \text{ mm} \times 3.0 \text{ mm}$ rectangular detection regions connected with a $200 \mu\text{m}$ trench. The image of the plasma ignited on this MGD clearly shows that the plasma "fills" out the trench area while it is confined in the edge of the pattern in the detection zones. When a piece of wax paper is treated using this MGD, the hydrophilic trench can be fabricated as expected. Only the peripheral region of the detection zone becomes hydrophilic. MGD with this pattern is therefore not suitable to make μ PADs.

To fabricate a MGD with suitable hydrophilic patterns for the μ PAD, a MGD with a 5×5 microplasma array with each spot $0.4 \text{ mm} \times 0.4 \text{ mm}$ was designed for the detection region. This device is then used to treat the wax paper to fabricate a μ PAD. The plasma visual appearance shown in Figure 3B demonstrates that uniform plasmas are ignited simultaneously in all 50 microcavities. An image with higher magnification is shown in Supporting Information Figure S4. The hydrophilic pattern defined using this MGD is favorable for μ PAD detection regions. A further test is performed making channels 200, 400, 600, and $800 \mu\text{m}$ wide on one MGD and using this MGD to fabricate a μ PAD. Figure 3C illustrates the results. It clearly shows that, for MGD with trenches $600 \mu\text{m}$ wide or narrower, a well-defined hydrophilic trench can be formed on

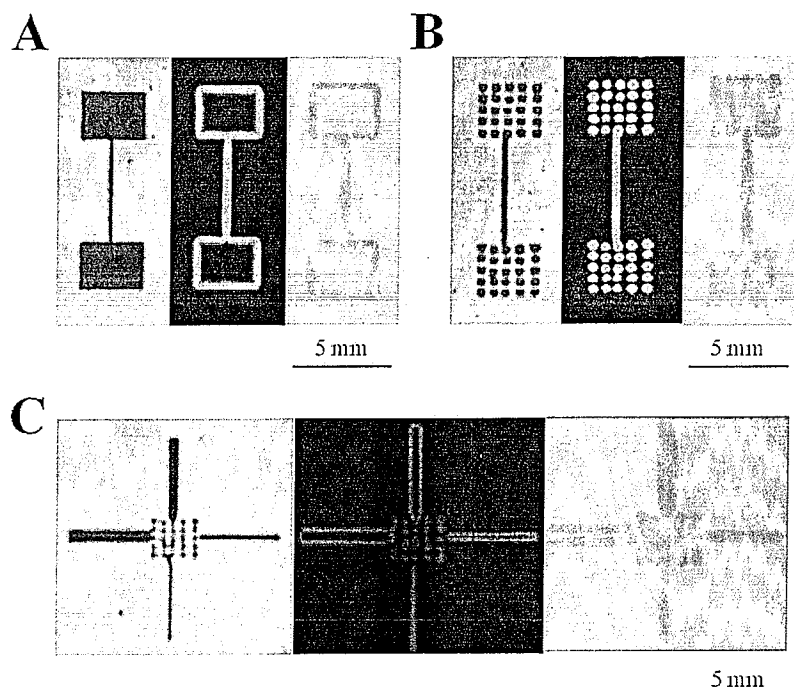


Figure 3. Effects of pattern-design on μ PAD characteristics. For each set of image, the left, center, and right panels are the visual appearance of the MGD, the MGD with plasma ignited, and the fabricated μ PAD, respectively. (A) The MGD pattern with two $2.5 \text{ mm} \times 3.0 \text{ mm}$ rectangular detection regions connected with a $200 \mu\text{m}$ trench. (B) The MGD pattern with two sets of 5×5 microplasma arrays with each spot $0.4 \text{ mm} \times 0.4 \text{ mm}$ connected with a $200 \mu\text{m}$ trench. (C) The MGD pattern with one 5×5 microplasma array in the middle and four trenches: 200, 400, 600, and $800 \mu\text{m}$ wide.

the wax paper. For MGD with a channel width of 800 micrometer, the hydrophilic channel splits into two. We note that channels 800 μm or wider can be fabricated in a rather straightforward manner by making two or more thinner channels in parallel.

It is shown in this figure that the plasma is not uniform. This is a result of the nonuniformity occurring in both the microscopic and macroscopic scales. In the microscopic scale, such a discharge is filamentary in nature; that is, the discharge consists of a great number of filaments several micrometers wide formed in a time scale of nanoseconds, as reported in the literature.³² For the nonuniformity in the macroscopic scale, it is caused by the nonuniform thickness of each layer of the CCL as well as the nonideal toner-transfer and etching processes, such as overetch or undercut during the etching step. The nonuniformity in the microscopic scale can be improved by properly adjust the operating condition, particularly using higher frequency or nanosecond pulsed power sources. More precise control in the MGD fabrication process can improve the nonuniformity in the macroscopic scale.

Assay Tests. To demonstrate that μPADs fabricated using the MGD-based process are suitable for quantitative biochemical analyses, we perform glucose and nitrite assays using these μPADs . Glucose and nitrite assays are both based on the colorimetric sensing mechanism. Detection regions are initially spotted by indicating reagents. After introducing sample solution onto the detection region, a chemical or an enzymatic reaction between the previously immobilized reagents and the sensing target compounds takes place and yields a color change. The glucose assay is based on the enzymatic oxidation of iodide to iodine. It yields a color change from clear to brown. This is one of the most used colorimetric reactions for μPADs demonstrated reported in the literature. We conduct this assay to demonstrate the practicality of our μPADs . In Figure 4, images of the glucose assay clearly show different color responses for analytes with different concentrations. The calibration curve shows a linear correlation for the concentration between 1 and 50 mM with an R^2 value 0.99705.

Nitrite was also chosen as the test assay, since it is a reliable biological marker for many human health conditions, such as periodontal disease.² We first applied 0.2 μL of nitrite indicator prior to spotting 1 μL of NaNO_2 solution with various concentrations onto the sampling zone. The color images of these tested μPADs are shown in Figure 5. The color responses in the detection regions are reasonably uniform, proving the performance in test solution transportation of our μPADs . Then, we analyzed the color responses of nitrite assays using image processing scheme II as described in the Experimental Section. The calibration curve shows a linear correlation with the analytes of concentrations between 0.1 and 5 mM with an R^2 value of 0.99706. The performances of glucose and nitrite assays clearly demonstrate that the proposed novel μPADs -fabricating technique via the MGD-based process is an ideal method to fabricate μPADs for monitoring people's health conditions.

CONCLUSION

We report the use of a printed circuit board fabrication-based process to fabricate MGDs in a rapid and cost-effective manner. The MGD can be operated under ambient air and is driven using a portable power source. The use of this MGD to fabricate μPADs is demonstrated. With a proper design of the MGD electrode geometry, μPADs with sub-millimeter channel

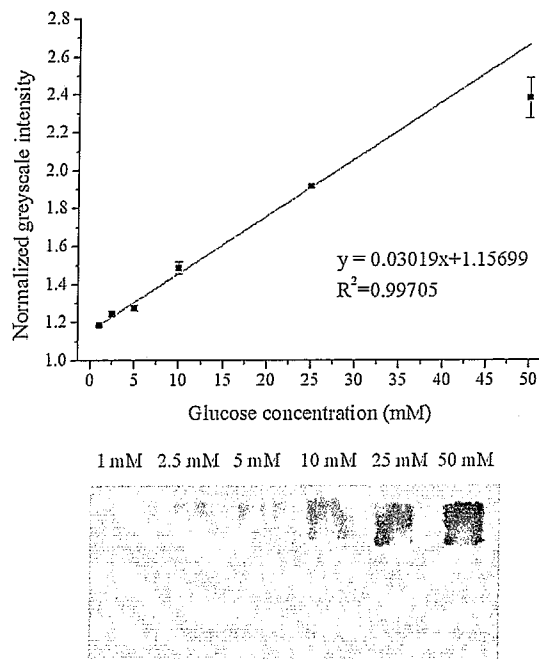


Figure 4. Calibration curve for glucose solution using image processing scheme I for color quantification. Color response of glucose assay on the patterned paper for a D-(+)-glucose concentration of 50, 25, 10, 5, 2.5, and 1 mM.

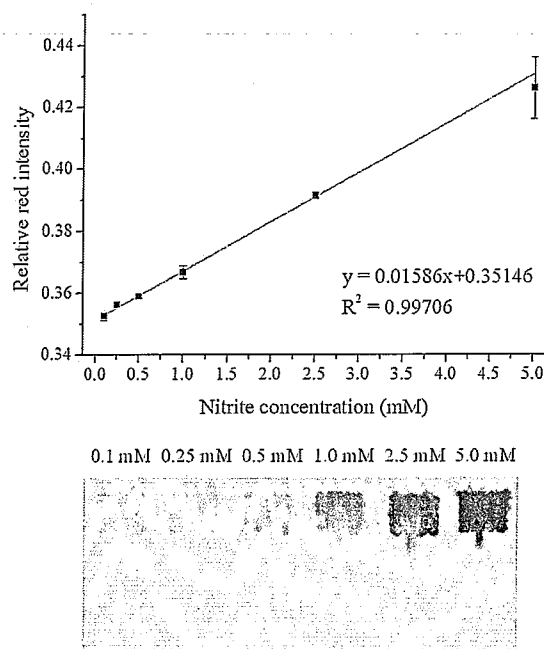


Figure 5. Calibration curve for nitrite solution using image processing scheme II for color quantification. Color response of nitrite assay on the patterned paper for NaNO_2 concentrations of 5, 2.5, 1, 0.5, 0.25, and 0.1 mM.

width can be fabricated within 1 min and with a total cost less than \$USD 0.05/device. This MGD possesses great flexibility, which could be a benefit for treating curved or nonflat surfaces. It could also extend the nature of this surface treatment process

from 2-dimensional to 3-dimensional and offers great possibilities for surfaces with various orientations. We also demonstrate that three types of hydrophobized paper, fluorocarbon paper, wax paper, and Double A paper, can be treated by MGD and form microfluidic channels in the paper platforms. We further investigate the relationship between MGD pattern-design and channel characteristics. The MGD pattern with two sets of 5×5 microplasma arrays with each spot $0.4 \text{ mm} \times 0.4 \text{ mm}$ connected with a $200\text{-}\mu\text{m}$ -wide trench was designed and was selected to fabricate our μPADs . Finally, we tested the μPADs by performing quantitative colorimetric assay tests and established calibration curves for detecting glucose and nitrite.

The cost-effective and portable features of the MGD make this MGD-based process a great candidate to fabricate μPADs in-field and/or on demand. The demonstration driving the MGD using a 12 V battery offers great possibilities under circumstances when μPADs are required to be fabricated in locations where stable electricity is not available. A great number of commercially available batteries deliver dc 12 V, such as lead-acid rechargeable batteries for automobiles. A typical battery of this type with a capacity of 45 amp-hour is sufficient to supply the MGD operation for at least 20 h. We believe this concept brings a leap to the fabrication and use of the impact of μPADs , which gives great impact in various applications, such as biomedical analysis, environmental monitoring, and food safety survey.

■ ASSOCIATED CONTENT

Supporting Information

Additional information as noted in text. This material is available free of charge via the Internet at <http://pubs.acs.org/>.

■ AUTHOR INFORMATION

Corresponding Author

*E-mail: chsu@ntu.edu.tw.

Notes

The authors declare no competing financial interest.

■ ACKNOWLEDGMENTS

This work is supported by the Ministry of Science and Technology, Taiwan (101-2221-E-002-163-MY2).

■ REFERENCES

- (1) Hsu, M. Y.; Yang, C. Y.; Hsu, W. H.; Lin, K. H.; Wang, C. Y.; Shen, Y. C.; Chen, Y. C.; Chau, S. F.; Tsai, H. Y.; Cheng, C. M. *Biomaterials* 2014, 35, 3729–3735.
- (2) Bhakta, S. A.; Borba, R.; Taba, M.; Garcia, C. D.; Carrilho, E. *Anal. Chim. Acta* 2014, 809, 117–122.
- (3) Hsu, C.-K.; Huang, H.-Y.; Chen, W.-R.; Nishie, W.; Ujue, H.; Natsuga, K.; Fan, S.-T.; Wang, H.-K.; Lee, J. Y.-Y.; Tsai, W.-L.; Shimizu, H.; Cheng, C.-M. *Anal. Chem.* 2014, 86, 4605–4610.
- (4) Lo, S. J.; Yang, S. C.; Yao, D. J.; Chen, J. H.; Tu, W. C.; Cheng, C. M. *Lab Chip* 2013, 13, 2686–2692.
- (5) Cheng, C. M.; Martinez, A. W.; Gong, J. L.; Mace, C. R.; Phillips, S. T.; Carrilho, E.; Mirica, K. A.; Whitesides, G. M. *Angew. Chem., Int. Ed.* 2010, 49, 4771–4774.
- (6) Martinez, A. W.; Phillips, S. T.; Butte, M. J.; Whitesides, G. M. *Angew. Chem., Int. Ed.* 2007, 46, 1318–1320.
- (7) Mentele, M. M.; Cunningham, J.; Koehler, K.; Volckens, J.; Henry, C. S. *Anal. Chem.* 2012, 84, 4474–4480.
- (8) Rattanarat, P.; Dungchai, W.; Cate, D.; Volckens, J.; Chailapakul, O.; Henry, C. S. *Anal. Chem.* 2014, 86, 3555–3562.
- (9) Hossain, S. M. Z.; Luckham, R. E.; McFadden, M. J.; Brennan, J. D. *Anal. Chem.* 2009, 81, 9055–9064.
- (10) Yetisen, A. K.; Akram, M. S.; Lowe, C. R. *Lab Chip* 2013, 13, 2210–2251.
- (11) Li, X.; Tian, J.; Nguyen, T.; Shen, W. *Anal. Chem.* 2008, 80, 9131–9134.
- (12) Kao, P.-K.; Hsu, C.-C. *Microfluid Nanofluid* 2014, 16, 811–818.
- (13) Carrilho, E.; Martinez, A. W.; Whitesides, G. M. *Anal. Chem.* 2009, 81, 7091–7095.
- (14) Zhang, Y.; Zhou, C. B.; Nie, J. F.; Le, S. W.; Qin, Q.; Liu, F.; Li, Y. P.; Li, J. P. *Anal. Chem.* 2014, 86, 2005–2012.
- (15) Abe, K.; Suzuki, K.; Citterio, D. *Anal. Chem.* 2008, 80, 6928–6934.
- (16) Cheng, C. M.; Mazzeo, A. D.; Gong, J. L.; Martinez, A. W.; Phillips, S. T.; Jain, N.; Whitesides, G. M. *Lab Chip* 2010, 10, 3201–3205.
- (17) Olkkonen, J.; Lehtinen, K.; Erho, T. *Anal. Chem.* 2010, 82, 10246–10250.
- (18) Bruzewicz, D. A.; Reches, M.; Whitesides, G. M. *Anal. Chem.* 2008, 80, 3387–3392.
- (19) Cassano, C. L.; Fan, Z. H. *Microfluid Nanofluid* 2013, 15, 173–181.
- (20) Liu, H.; Crooks, R. M. *Anal. Chem.* 2012, 84, 2528–2532.
- (21) Kakei, R.; Ogino, A.; Iwata, F.; Nagatsu, M. *Thin Solid Films* 2010, 518, 3457–3460.
- (22) Becker, K. H.; Schoenbach, K. H.; Eden, J. G. *J. Phys. D: Appl. Phys.* 2006, 39, R55–R70.
- (23) Szili, E. J.; Al-Bataineh, S. A.; Ruschitzka, P.; Desmet, G.; Priest, C.; Griesser, H. J.; Voelcker, N. H.; Harding, F. J.; Steele, D. A.; Short, R. D. *RSC Adv.* 2012, 2, 12007–12010.
- (24) Yang, Y. J.; Hsu, C. C. *J. Microelectromech. Syst.* 2013, 22, 256–258.
- (25) Kim, S. J.; Chung, T. H.; Bae, S. H.; Leem, S. H. *Appl. Phys. Lett.* 2009, 94, 141502.
- (26) Symonds, J. M.; Galhena, A. S.; Fernandez, F. M.; Orlando, T. M. *Anal. Chem.* 2010, 82, 621–627.
- (27) Weagant, S.; Chen, V.; Karanassios, V. *Anal. Bioanal. Chem.* 2011, 401, 2865–2880.
- (28) Hsu, C. C.; Tsai, J. H.; Yang, Y. J.; Liao, Y. C.; Lu, Y. W. *J. Microelectromech. Syst.* 2012, 21, 1013–1015.
- (29) Tachibana, K. *IEE J. Trans. Electrical Electronic Eng.* 2006, 1, 145–155.
- (30) Karanassios, V. *Spectrochim. Acta, Part B: At. Spectrosc.* 2004, 59, 909–928.
- (31) Gibalov, V. I.; Pietsch, G. J. *J. Phys. D: Appl. Phys.* 2000, 33, 2618–2636.
- (32) Kogelschatz, U. *Plasma Chem. Plasma Process.* 2003, 23, 1–46.
- (33) Garnier, G.; Wright, J.; Godbout, L.; Yu, L. *Colloids Surf., A* 1998, 145, 153–165.
- (34) Li, X.; Tian, J.; Shen, W. *Cellulose* 2010, 17, 649–659.
- (35) Klasner, S. A.; Price, A. K.; Hoeman, K. W.; Wilson, R. S.; Bell, K. J.; Culbertson, C. T. *Anal. Bioanal. Chem.* 2010, 397, 1821–1829.
- (36) Martinez, A. W.; Phillips, S. T.; Carrilho, E.; Thomas, S. W.; Sindi, H.; Whitesides, G. M. *Anal. Chem.* 2008, 80, 3699–3707.
- (37) Blicharz, T. M.; Rissin, D. M.; Bowden, M.; Hayman, R. B.; DiCesare, C.; Bhatia, J. S.; Grand-Pierre, N.; Siqueira, W. L.; Helmerhorst, E. J.; Loscalzo, J.; Oppenheim, F. G.; Walt, D. R. *Clin. Chem.* 2008, 54, 1473–1480.